Picosecond soliton transmission by use of concatenated gain-distributed nonlinear amplifying fiber loop mirrors

Wen-hua Cao and Ping Kong A. Wai

Stable picosecond soliton transmission is demonstrated numerically by use of concatenated gain-distributed nonlinear amplifying fiber loop mirrors (NALMs). We show that, as compared with previous soliton transmission schemes that use conventional NALMs or nonlinear optical loop mirror and amplifier combinations, the present scheme permits a significant increase of loop-mirror (amplifier) spacing. The broad switching window of the present device and the high-quality pulses switched from it provide a reasonable stability range for soliton transmission. We also show that a soliton self-frequency shift can be suppressed by the gain-dispersion effect in the amplifying fiber loop and that soliton–soliton interactions can be partially reduced by using lowly dispersive transmission fibers.

OCIS codes: 060.5530, 060.2330, 060.4370, 060.1810.

1. Introduction

Soliton communication systems are leading candidates for long-haul light-wave transmission links because they offer the possibility of a dynamic balance between group-velocity dispersion (GVD) and self-phase modulation, the two effects that severely limit the performance of nonsoliton systems.[1] Most system experiments employ the technique of lumped amplification and place fiber amplifiers periodically along the transmission line to compensate fiber loss. The principal concept that has emerged in the context of lumped amplification is the path-average or guiding-center solitons.[2,3] Their use allows propagation of solitons through lossy fibers provided that the amplifier spacing L_A is short compared with the dispersion length L_D. However, since L_D is proportional to the square of the soliton width, the condition $L_A < L_D$ results in unreasonably short amplifier spacing if the soliton width reduces to a few picoseconds. Several schemes have been proposed to design soliton communication systems that can operate beyond the path-average-soliton regime. They include the dynamic soliton propagation technique,[4] the introduction of a generalized saturable absorber in the transmission line,[5] the use of nonlinear optical loop mirrors (NOLMs)[6] or nonlinear amplifying fiber loop mirrors (NALMs),[7,8] and the use of prechirped optical pulses.[9,10] Among them the use of NOLMs or NALMs has been shown to result in the largest L_A to L_D ratio. However, the amplifier spacing, i.e., the loop-mirror spacing,[6–8] is still short. For 1.5 ps soliton transmission, the loop-mirror spacing is only 10 km.

Recently,[11] we studied the self-switching of ultrashort solitons in a NALM that has a gain uniformly distributed around its whole loop length. The switching performance of this NALM was compared to those of the NOLM and the conventional NALM (with a lumped gain placed at a specific point in the loop). It was shown that, as compared with a conventional NALM or a NOLM, a gain-distributed NALM can produce higher-quality pulses and permits more efficient pulse compression. It was also shown that the gain-distributed NALM has additional advantages over the conventional NALM, such as sharpened switching edges, a flattened switching peak, and robustness to gain variations. In this paper, we numerically demonstrate that the loop-mirror spacing of the soliton transmission schemes described in Refs. 6–8 can be significantly increased if gain-distributed NALMs are used instead of the conventional NALMs or the NOLM and amplifier combinations. The broad switching window of the present device and the high-quality pulses switched from it provide a reasonable stability range for soliton transmission. We also show

The authors are with Photonics Research Center and Department of Electronic and Information Engineering, Hong Kong Polytechnic University, Hung Hom, Hong Kong. W. Cao's e-mail address is wwhhcao@163.com.

Received 28 January 2005; revised 21 June 2005; accepted 26 June 2005.

0003-6935/05/357611-10$15.00/0

that the soliton self-frequency shift can be suppressed by the gain-dispersion effect in the gain-distributed NALM and that soliton–soliton interactions can be partially reduced by using lowly dispersive transmission fibers. Note that our previous studies[12] have addressed the use of the gain-distributed NALM to simultaneously amplify and compress ultrashort fundamental solitons.

2. Basic Equations

We assume that the gain-distributed NALM is constructed by connecting a piece of erbium-doped fiber (with uniform gain) to the two output ports of a fiber coupler. For simulations of pulse evolution in an erbium-doped fiber, we use the split-step Fourier method to solve a generalized nonlinear Schrödinger equation that takes the form[12,13]

$$i\frac{\partial u}{\partial \xi}+\frac{1}{2}(1-id)\frac{\partial^2 u}{\partial \tau^2}+|u|^2u = \frac{i}{2}\mu u+i\delta\frac{\partial^3 u}{\partial \tau^3}+\tau_R u\frac{\partial |u|^2}{\partial \tau}, \quad (1)$$

where ξ, τ, and $u(\xi, \tau)$ are the normalized distance, time, and pulse envelope in soliton units, respectively. The parameters μ, d, τ_R, and δ account for, respectively, the effects of gain, gain dispersion, Raman self-scattering (RSS), and third-order dispersion (TOD). In real parameters

$$\xi=\frac{z}{L_D}=\frac{z|\beta_2|}{{T_0}^2},\quad \tau=\frac{t-z/v_g}{T_0},\quad d=g_0L_D\frac{{T_2}^2}{{T_0}^2}, \quad (2)$$

$$\mu=(g_0-\alpha)L_D,\quad \delta=\frac{\beta_3}{6|\beta_2|T_0},\quad \tau_R=\frac{T_R}{T_0}, \quad (3)$$

where T_0 is the half width (at the $1/e$ intensity point) of the input pulse, v_g is the group velocity, β_2 is the GVD coefficient, β_3 is the TOD coefficient, T_R is the Raman resonant time constant, α is the fiber loss, T_2 is the dipole relaxation time, g_0 is the unsaturated gain, and $L_D={T_0}^2/|\beta_2|$ is the dispersion length. We do not include self-steepening and two-photon absorption effects since they play much smaller roles when compared with the other effects.

The input pulse is assumed to be

$$u(0,\tau)=A\,\mathrm{sech}(\tau), \quad (4)$$

where the parameter A is usually called soliton order (although sometimes it may not be an integer) and is related to the physical parameters by

$$A^2=\frac{\gamma P_0{T_0}^2}{|\beta_2|}. \quad (5)$$

The parameter γ is the nonlinearity coefficient and P_0 is the peak power of the input pulse. Equation (1) can also describe pulse evolution in a passive fiber when the gain and gain-dispersion terms are excluded.

3. Switching Characteristics of Nonlinear Optical Loop Mirrors and Nonlinear Amplifying Fiber Loop Mirrors

Before we investigate soliton transmission, it is useful to compare the switching characteristics of a gain-distributed NALM to those of a conventional NALM and a NOLM and amplifier combination. In all cases, we neglect the amplifier noise in our simulations. The input pulse width is assumed to be the same, i.e., $T_{\mathrm{FWHM}}=5$ ps ($T_0\approx 2.836$ ps), the fiber parameters are $\beta_2=-20$ ps^2/km and $\gamma=5$ W^{-1} km^{-1}, and the loop length is fixed at πL_D ($\sim$1.26 km). We temporarily neglect the effects of gain dispersion, RSS, and TOD because they have negligible influence on the switching characteristics for an input pulse as wide as 5 ps. Fiber loss is included with $\alpha=0.046$ km^{-1} (i.e., 0.2 dB/km) in the cases of a conventional NALM and NOLM and amplifier combinations.

Figures 1(a) and 1(b) show, respectively, the switching characteristics of a conventional NALM with a lumped gain of 5 and 10 dB. For each case, the coupler is symmetric with a power-splitting ratio of 50:50 and the amplifier is placed within the loop immediately after the coupler. The solid, dashed, and dashed–dotted curves show, respectively, the dependence of the loop transmission, the pedestal energy, and the time–bandwidth product ($\Delta\nu\Delta\tau\times 100$) of the transmitted pulse on the peak power of the input pulse. The horizontal dotted line in each case shows the time–bandwidth product of 0.315($\times$100) of a transform-limited hyperbolic-secant pulse. Here the transmission is defined as the ratio of the transmitted (switched) energy to the sum of the transmitted and reflected energies. In the definition of the time–bandwidth product, $\Delta\nu$ and $\Delta\tau$ represent, respectively, the spectral full width at half-maximum (FWHM) and temporal FWHM of the transmitted pulse. The pedestal energy is defined as the relative difference between the total energy of the transmitted pulse and the energy of a hyperbolic-secant pulse having the same peak power and width as those of the transmitted pulse, i.e.,

$$\text{Pedestal energy }(\%)=\frac{|E_{\mathrm{total}}-E_{\mathrm{sech}}|}{E_{\mathrm{total}}}\times 100\%. \quad (6)$$

Note that the energy of a hyperbolic-secant pulse with peak power P_{peak} and pulse width T_{FWHM} is given by

$$E_{\mathrm{sech}}=2P_{\mathrm{peak}}\frac{T_{\mathrm{FWHM}}}{1.763}. \quad (7)$$

Figures 1(c) and 1(d) show the compression factor (solid curve) and the soliton order (dashed curve) of the transmitted pulses corresponding, respectively, to Figs. 1(a) and 1(b), where the compression factor is defined as the ratio of the T_{FWHM} of the input pulse to

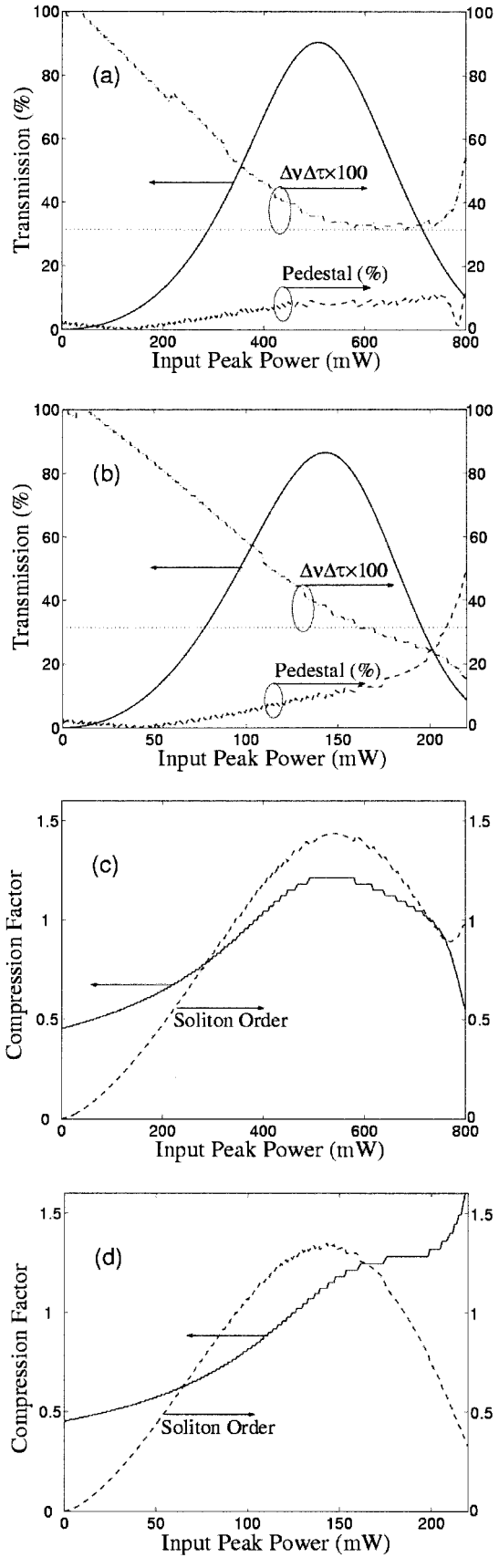

Fig. 1. Switching characteristics of a conventional NALM: (a), (c) with a lumped gain of 5 dB; (b), (d) with a lumped gain of 10 dB, where $\Delta\nu\Delta\tau$ is the time–bandwidth product of the transmitted pulse.

that of the transmitted pulse, and the soliton order is estimated from the peak power and width of the transmitted pulse. We see that the conventional NALM exhibits a sinusoidal transmittance with slow switching transitions near the switching edges, which is a disadvantage for all-optical ultrafast digital signal processing. The qualities of the transmitted pulses around the transmission peak are poor since the pulses are chirped and are accompanied by nonnegligible pedestals (>10%). The compression factor around the transmission peaks is kept below 1.5 and seems to be insensitive to the amplifier gain. Although the soliton orders are close to those of fundamental solitons, the transmitted pulses do not actually retain the characteristics of fundamental solitons because they are chirped and are accompanied by pedestals.

Figure 2 shows the switching characteristics of the NOLM and amplifier combination, where Figs. 2(a) and 2(c) correspond to the case in which the coupler has a power-splitting ratio of 56:44 (which is the typical value used for the gain-distributed NALM discussed later), and Figs. 2(b) and 2(d) correspond to the case in which the coupler has a power-splitting ratio of 60:40. In both cases, the same lumped gain of 10 dB is placed at the input port (outside the loop). It is seen that, as compared with the conventional NALM, the NOLM and amplifier combination exhibits a sharpening of the switching transition as well as a flattening of the switching peak [see Fig. 2(b)]. The compression factor is slightly larger than that provided by the conventional NALM. In fact, the coupler power-splitting ratio of 60:40 used for Figs. 2(b) and 2(d) is almost the best one in respect of the transmission and the pedestal energy. However, in most cases the transmitted pulses are not close to transform-limited pulses. Simulations not shown here indicate that when the time–bandwidth product of the transmitted pulse drops below or increases above 0.315, the transmitted pulse deviates from the sech pulse and is chirped. When the time–bandwidth product drops below 0.315, the transmitted pulse is positively chirped, whereas when the time–bandwidth product increases above 0.315, the transmitted pulse is negatively chirped.

The results are quite different if we place a distributed gain instead of a lumped gain in the loop. Figure 3 shows the switching characteristics of the gain-distributed NALM under conditions identical to those of Figs. 1(b) and 1(d) except that the 10 dB gain is uniformly distributed along the loop and that the coupler is asymmetric with power-splitting ratios of 54:46 for Figs. 3(a) and 3(c) and 56:44 for Figs. 3(b) and 3(d). As compared to the two cases discussed above, we see that distributed gain causes a significant improvement in the quality of the transmitted pulse. Here, the pedestals of the transmitted pulses are very small (less than 5%) and the transmitted pulses are very close to transform-limited pulses. Another difference is that the gain-distributed NALM permits more significant pulse compression than the conventional NALM or the NOLM and amplifier com-

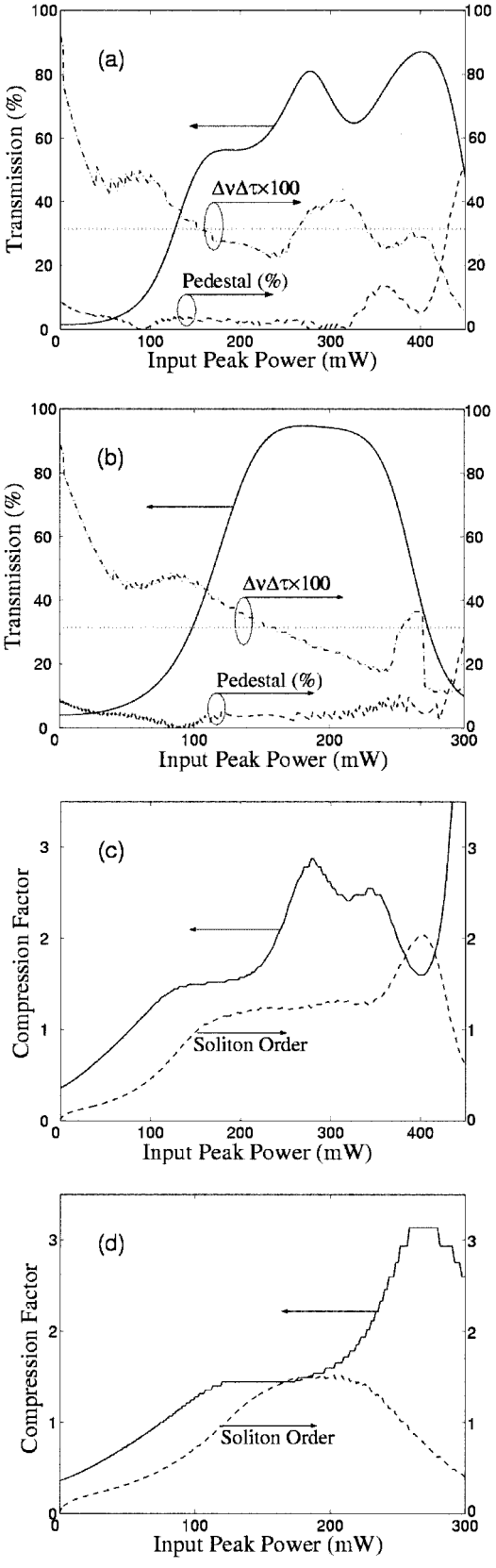

Fig. 2. Switching characteristics of a NOLM and amplifier combination: (a), (c) the coupler has a power-splitting ratio of 56:44; (b), (d) the coupler has a power-splitting ratio of 60:40. In each case, a lumped gain of 10 dB is placed at the input port (outside the NOLM), where $\Delta\nu\Delta\tau$ is the time–bandwidth product of the transmitted pulse.

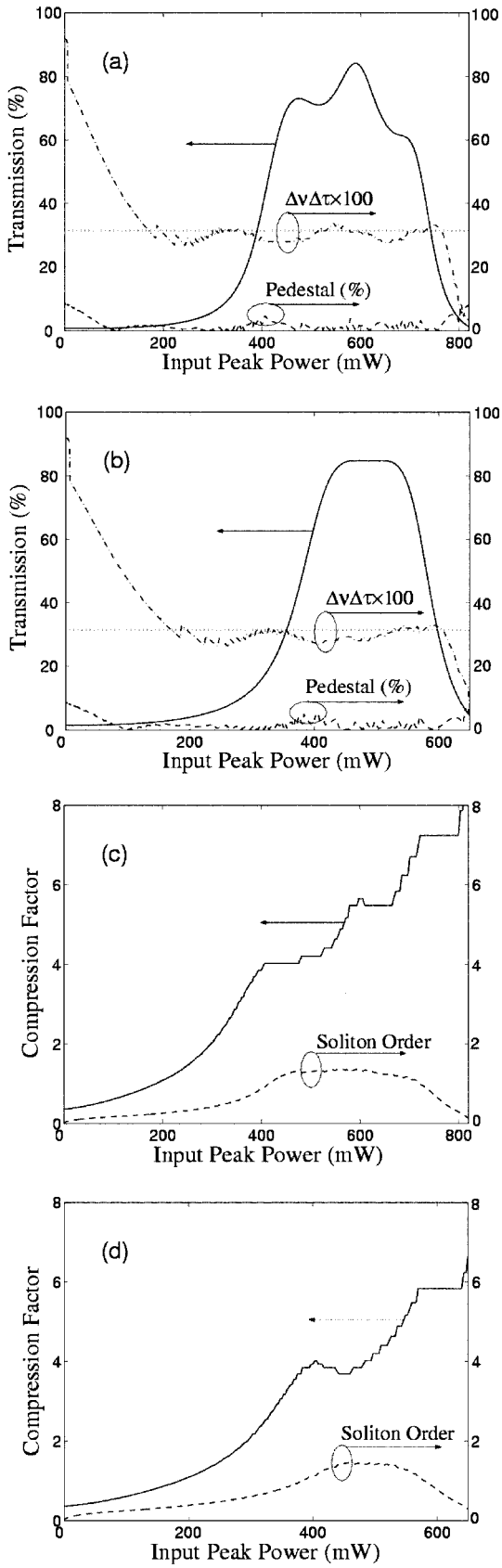

Fig. 3. Switching characteristics of a gain-distributed NALM with a gain of 10 dB: (a), (c) the coupler has a power-splitting ratio of 54:46; (b), (d) the coupler has a power-splitting ratio of 56:44, where $\Delta\nu\Delta\tau$ is the time–bandwidth product of the transmitted pulse.

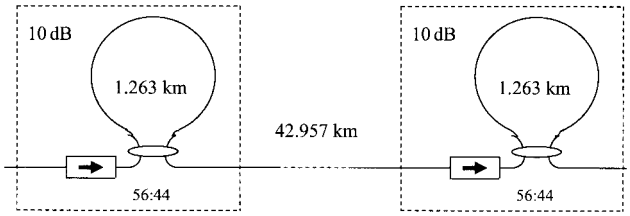

Fig. 4. Schematic diagram of the soliton transmission line.

bination. This compression nature will be very effective for compensating fiber-loss-induced soliton broadening and is really the motivation for our attempting to use a gain-distributed NALM to increase the amplifier spacing of a soliton transmission system.

The different performance between the gain-distributed NALM and the conventional NALM or the NOLM and amplifier combination can be understood as follows. In the case of the conventional NALM, one of the counterpropagating pulses in the loop experiences compression while the other experiences broadening because the amplifier is asymmetrically placed. Thus a serious mismatch of pulse shapes occurs when the two pulses recombine at the coupler. The situation is the same for the NOLM and amplifier combination because of the asymmetric coupler. Whereas, in the case of the gain-distributed NALM, both the clockwise and counterclockwise pulses experience compression because of the distributed gain. Thus, unlike the other two cases, serious mismatch of the counterpropagating pulse shapes in the gain-distributed NALM is prevented, leading to more complete interference when the two pulses recombine at the coupler.

4. Soliton Transmission Using Gain-Distributed Nonlinear Amplifying Fiber Loop Mirrors

A. Demonstration of the Technique

Figure 4 shows the transmission scheme that is similar to that adopted in Ref. 6 except that gain-distributed NALMs are used instead of the NOLM and amplifier combination. The gain-distributed NALM is identical to that used for Figs. 3(b) and 3(d) and is inserted periodically in the transmission link. The coupler power-splitting ratio of the gain-distributed NALMs is chosen to be 56:44 so that the switching window is flat and smooth, and the switched pulse has a higher quality as seen from Figs. 3(b) and 3(d). To provide a uniform gain along the entire loop length, the loop can be pumped simultaneously in both clockwise and counterclockwise directions using two semiconductor lasers located at the two ends of the loop. At the input of each loop mirror, an optical isolator is placed to absorb any pulse components reflected from the loop mirror. The parameters β_2 and γ of the transmission fiber are identical to those of the fiber loop, and the transmission fiber loss is 0.2 dB/km. Pulse propagation within both the NALM and the transmission fiber is modeled by the numerical integration of Eq. (1) while temporarily neglecting the effects of gain dispersion, RSS, and TOD.

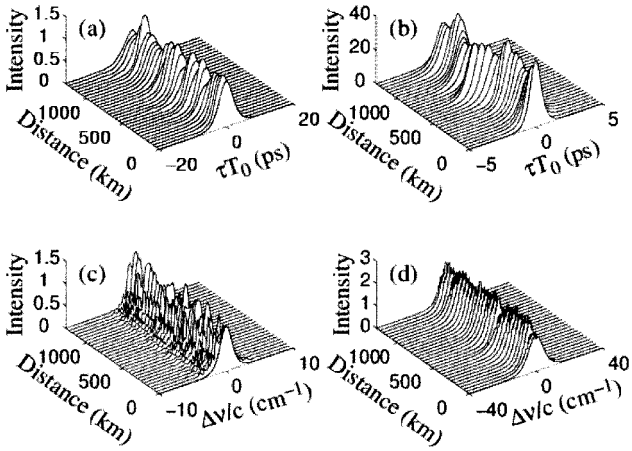

Fig. 5. Pulse shape and spectral evolution through a transmission fiber link with concatenated gain-distributed NALMs, where (a) and (c) are measured at the inputs of the NALMs and (b) and (d) are measured at the outputs of the NALMs.

Figure 5 shows soliton transmission over 1288.71 km with a loop-mirror spacing of 42.957 km, where the input pulse to the first NALM is 1.05 sech(τ) with $P_0 = 548.3$ mW and $T_{\mathrm{FWHM}} = 5$ ps, which is close to a fundamental soliton. The loop length is fixed at πL_D ($\sim$1.263 km), and the first NALM is set to operate at a switching point slightly past its switching peak. Figures 5(a) and 5(b) show the pulse shapes measured, respectively, at the input and output of each NALM, and Figs. 5(c) and 5(d) show the spectra of the pulses corresponding, respectively, to Figs. 5(a) and 5(b). The intensities of the pulse shapes and spectra are normalized, respectively, to the peak intensities of the input pulse shape and spectrum. We see that the input pulse is amplified and compressed with a compression ratio of approximately 4 when it is switched by the NALM every time. The dispersive waves or noise and continuum around the input pulse are suppressed by the NALM. The switched pulse is close to a fundamental soliton but with higher energy than that of the input pulse. Transmission loss attenuates the pulse energy and broadens its width, and the pulse is nearly recovered after it passes through the next NALM. We see that although the pulse intensity varies at the input of each NALM, it does not affect the periodic transmission because the NALM provides a negative feedback mechanism as analyzed in Refs. 6 and 8. Figure 5(c) shows that, at the input of each NALM, sidebands are formed because the pulse transmitted from the former NALM is not exactly a fundamental soliton and emits dispersive waves when it propagates in the transmission fiber. The dispersive waves lead to the generation of the spectral sidebands. The sidebands are significantly suppressed and the soliton nature of the pulse is nearly recovered when it passes through the NALM every time as shown in Fig. 5(d). Note

that the 10 dB gain incorporated in each NALM is larger than that needed to balance the transmission loss; the residual gain is consumed by the reflection of the NALM. We have assumed that any pulse components reflected back up the input are absorbed by optical isolators. We have also assumed lossless couplers and lossless splices.

It should be pointed out that the nonlinearity coefficient γ assumed for the transmission fiber is larger than that of most telecommunication fibers. However, the choice of a particular γ value should not affect the demonstration of the transmission scheme because all figures above will remain the same if we decrease the γ of both the NALMs and the transmission fibers from 5 to 2 W^{-1} km^{-1} (which is the typical γ value of most telecommunication fibers) while increasing the input peak power to the first NALM by a factor of 2.5. Choosing a larger γ has two advantages. First, as seen from Eq. (5), the required soliton peak power is inversely proportional to γ. And second, for a fixed switching power, the length of the NALM decreases as the parameter γ increases.

One may feel that the comparison of the present loop-mirror spacing of 42.957 km to those achieved in Refs. 6 and 8 (where it was about 6–15 km) is unfair because the initial pulse width of 5 ps assumed here is larger than that assumed in Refs. 6 and 8 (where it was 1.5 ps). However, the loop-mirror spacing is determined by the gain rather than the initial pulse width. Our simulations (not shown here) indicate that, for the same gain of 10 dB, the loop-mirror spacing is nearly the same as that of Fig. 5 when the initial pulse width is 2 ps provided that the soliton order A of the input pulse is the same as that assumed for Fig. 5 and that the loop length is decreased to 0.202 km ($\sim \pi L_D$) so that the NALM has the same switching window as before and operates at the same switching point.

The reason for the small loop-mirror spacings achieved in Refs. 6 and 8 is that the amplifier gain incorporated there cannot be too large; otherwise, pulse cannot be periodically recovered because the adiabatic nature of the loop mirrors used there decreases as gain increases.[14] Figure 6(a) shows the evolution of the normalized peak intensity and normalized width of a switched pulse from a conventional NALM in a transmission fiber with parameters β_2 and γ assumed earlier, where the NALM contains a lumped gain of 10 dB [i.e., its switching window is identical to that shown in Fig. 1(b)] and operates at its transmission peak. The peak intensity and width are normalized, respectively, to the peak intensity and width of the input pulse to the NALM. We see that, at any point of the transmission fiber, the pulse intensity and width cannot simultaneously match with those of the input pulse. For example, at the cross point, both the intensity and width are 1.5 times larger than those of the input pulse. This implies that periodic transmission is impossible under this case. This is why an additional coupler must be spliced to the output of the main coupler as described in Ref. 8,

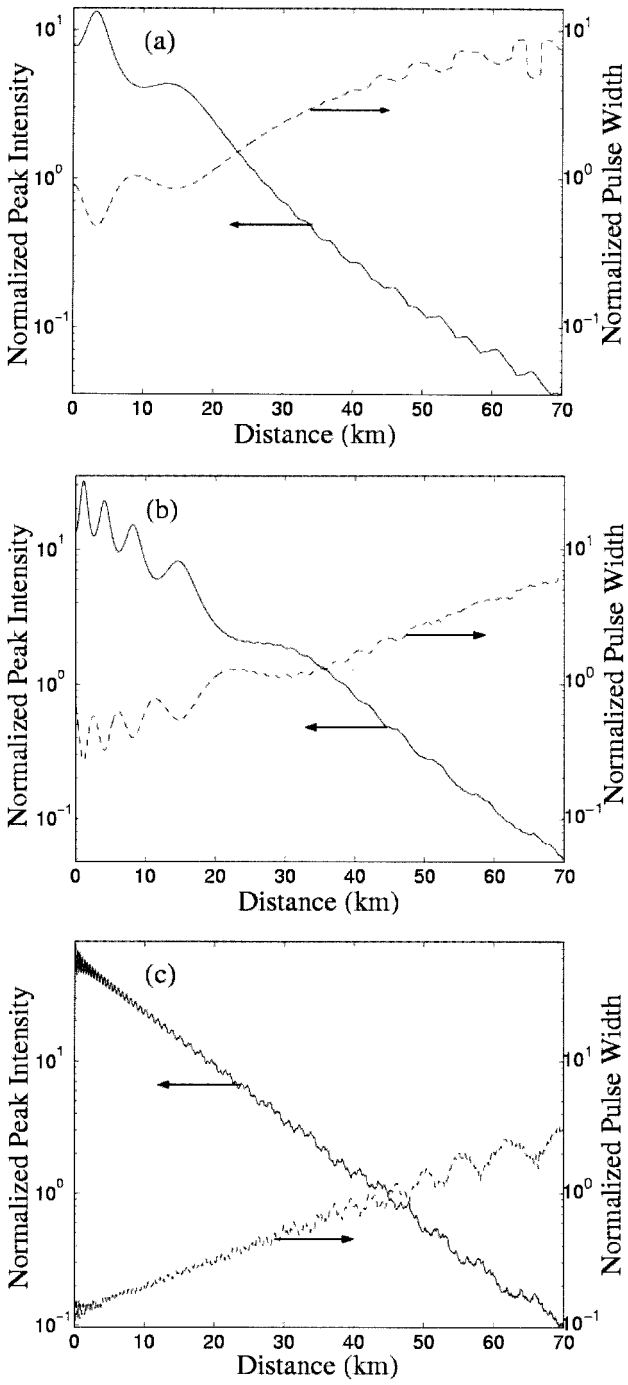

Fig. 6. Evolution of the normalized peak intensity and normalized width of pulses switched from (a) the conventional NALM, (b) the NOLM and amplifier combination, and (c) the gain-distributed NALM.

where a 7 dB gain is introduced within the loop. At the same time, an additional 3 dB coupler is spliced to the output of the main coupler to attenuate the pulse amplitude so that periodic pulse recovery can be guaranteed for stable transmission. Thus the net gain provided by the NALM is only 4 dB, which results in a loop-mirror spacing of 14 km.

The situation is nearly the same in the case of a

NOLM and amplifier combination, which is illustrated by Fig. 6(b). Where the switching window is the same as shown by Fig. 2(b), i.e., the coupler has a power-splitting ratio of 60:40 and a lumped amplifier with 10 dB gain is placed between the input pulse and the NOLM that operates at its transmission peak. In this case, recovery of the input pulse is also impossible. At the cross point, both the intensity and width are 1.3 times larger than those of the input pulse. We have adjusted the loop length and the coupler power-splitting ratio while letting the NOLM operate at its transmission peak and found that the input pulse cannot be recovered in any case. However, the situation is different in the case of a gain-distributed NALM, which is shown by Fig. 6(c). Where the input pulse and the gain-distributed NALM are identical to those used for Fig. 5. We see that, as the propagation continues, the pulse intensity decreases and the pulse width increases, both in an exponential manner. At the cross point, the pulse intensity and width simultaneously match with those of the input pulse.

B. Soliton–Soliton Interactions

A well-known aspect of solitons' behavior is their mutual interactions, of which two forms have been observed, i.e., short-range phase-dependent interaction and long-range phase-independent interaction. In the short-range interaction, solitons are spaced 1–6 soliton widths apart. In this case, if a pair of solitons are initially in phase with the same amplitude, they perform a mutual oscillation, periodically coalescing and then separating again. A pair of out-of-phase solitons separate from each other after an initial attraction stage. The strength of these interactions decreases exponentially with initial soliton separation. Long-range interaction takes place when the initial solitons are spaced many soliton widths apart,[15] which is independent of the initial phase, being dependent on the initial soliton separation.

Figure 7(a) shows soliton–soliton interaction under conditions identical to those of Fig. 5 except that two in-phase solitons with an initial separation of 30 ps are considered, where each curve represents the pulse shape at the input of each NALM. The two solitons reveal mutual repulsion, resulting in a separation of approximately 80 ps at 430 km. This is a long-range interaction because the initial soliton separation is about 15 times larger than the average soliton width along the transmission line (considering that the NALM provides a pulse compression factor of about 4). Similar to that described in Ref. 6, we observed both repulsion and attraction of the solitons by adjusting the initial soliton separation.

The interaction, which may be caused by the dispersive background waves[15] or the acoustic shock-wave-induced electrostriction in optical fibers,[16] is detrimental to a soliton communication system. It can be partially suppressed by using lowly dispersive fibers to increase the dispersion length as shown in Fig. 7(b), where β_2 of both the loop mirror and the transmission fiber is reduced to -10 ps^2/km. Correspondingly, the loop length is increased to 2.526 km and the peak power of the input soliton is decreased to 274.1 mW so that the NALM has the same switching window as before and operates at the same switching point. We have attempted to decrease β_2 to -5 ps^2/km to further suppress soliton interaction, but the soliton cannot be periodically recovered. The reason is that the pulse switched by the NALM contains nonsoliton components, so the ratio of the loop-mirror spacing L_A to the dispersion length L_D should be large enough that the pulse can evolve into a fundamental soliton before arriving at the input port of the next NALM.

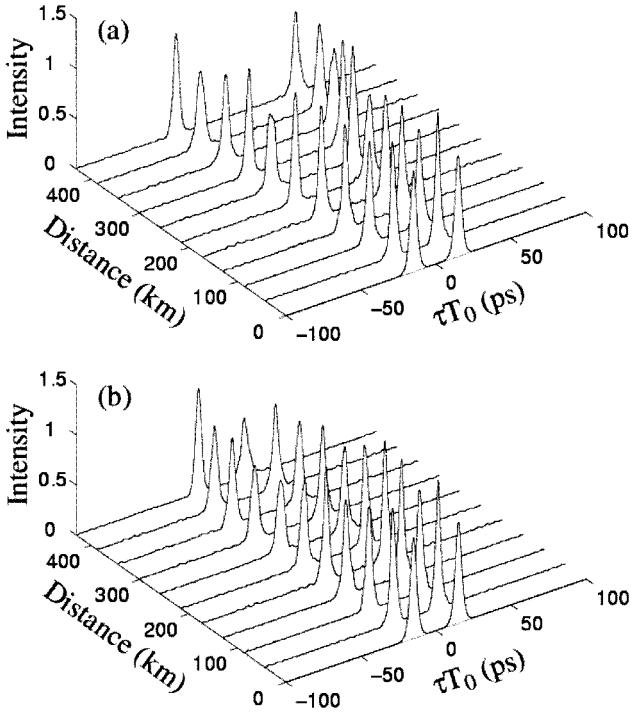

Fig. 7. Interaction of two in-phase solitons initially separated by 30 ps: (a) $\beta_2 = -20$ ps^2/km, (b) $\beta_2 = -10$ ps^2/km.

C. Effect of Raman Self-Scattering

The results presented thus far were obtained without consideration of higher-order effects such as RSS, TOD, and pulse self-steepening. It is known that RSS is the most harmful effect for long-distance transmission of picosecond solitons, whereas the effects of TOD and self-steepening are important only when the pulse wavelength is close to the zero-dispersion wavelength of the fiber or the pulse width is shorter than 0.1 ps. In this subsection, we consider how RSS affects soliton transmission and how this effect can be controlled.

Figure 8 shows spectra evolution under conditions identical to those used for Fig. 5 except that the RSS effect is considered, where Figs. 8(a) and 8(b) show the pulse spectra measured, respectively, at the input and output of each NALM. We see that RSS leads to a significant downshift of the optical carrier fre-

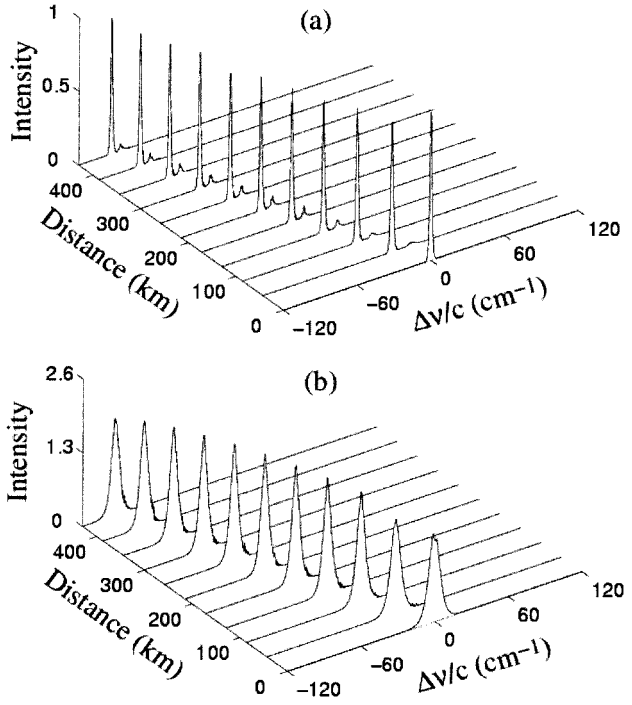

Fig. 8. Spectra evolution under conditions identical to those used for Fig. 5 except that the RSS effect is considered, where (a) and (b) show the pulse spectra measured, respectively, at the input and output of each NALM.

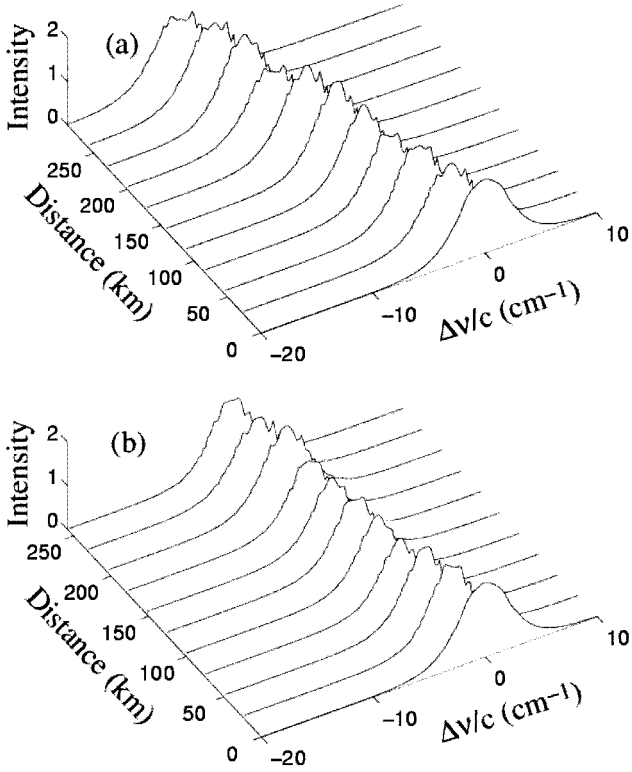

Fig. 9. Soliton spectra measured at the output of each NALM when (a) only the RSS effect is considered and (b) both the RSS effect and the gain-dispersion effect are considered. In both cases, the NALM has a distributed gain of 7.1 dB and the loop length is 2.526 km.

quency through the soliton self-frequency shift.[17] For a transmission distance of 430 km, the center frequency shifts by 3000 GHz, which corresponds to a wavelength redshift of 24.4 nm if the center wavelength of the input pulse is 1550 nm. This is deleterious because the pulse spectrum will walk out from under the NALMs gain bandwidth. As a result, the pulse energy switched by the NALM becomes smaller and smaller until eventually it ceases to pass through the NALM and the transmission breaks down.

The RSS-induced soliton self-frequency shift may be suppressed by the NALM because of the gain-dispersion effect[18] along the loop. Physically, this can be understood by noting that a shift of the soliton spectrum from the gain peak reduces the gain experienced by the center frequency of the soliton. At the same time, spectral components located near the gain peak are amplified more. Thus, the NALM has a built-in mechanism that tries to pull the soliton spectrum toward the gain peak, resulting in a decrease of the soliton self-frequency shift. We made an attempt to demonstrate this mechanism under conditions identical to those of Fig. 8 by simultaneously considering RSS and gain dispersion in the loop, but the soliton decayed after the second NALM. The reason is that the spectrum shift between two neighboring NALMs is so large that a significant portion of the spectrum shifts away from the gain peak, resulting in a significant decrease of gain experienced by the soliton. One possible solution[6] is to insert narrow-bandwidth filters between neighboring NALMs. In this case, the filter will provide an additional force to pull the soliton spectrum toward the gain peak. Thus, the spectrum shift between two neighboring NALMs is reduced so that gain dispersion in the loop can periodically balance the residual spectrum shift. Of course, the gain of each NALM should be slightly increased to compensate for the filter-induced energy loss.

An alternative solution without use of filters is to decrease the loop-mirror spacing by introducing a smaller gain within the NALM, so it is necessary to modify the structure of the gain-distributed NALM used for Fig. 8. The modification is simple and is as follows. The total gain around the loop is decreased to 7.1 dB while the loop length is increased to 2.526 km (i.e., twice as long as that assumed earlier). The parameters β_2 and γ of both the loop and the transmission fiber remain unchanged, and the input pulse and the coupler power-splitting ratio are identical to those used for Fig. 8. In this case, the loop-mirror spacing is reduced to 28.94 km. Figure 9(a) shows the soliton spectra measured at the output of each NALM when only the RSS effect is considered (without consideration of the gain-dispersion effect). We see that the spectrum shift between two neighboring NALMs is much smaller as compared with the case shown by Fig. 8. For a transmission distance of 289.4 km, the center frequency shifts only by 300 GHz. This benefits from the fact that reducing the gain of the NALM not only decreases the loop-mirror spacing but also

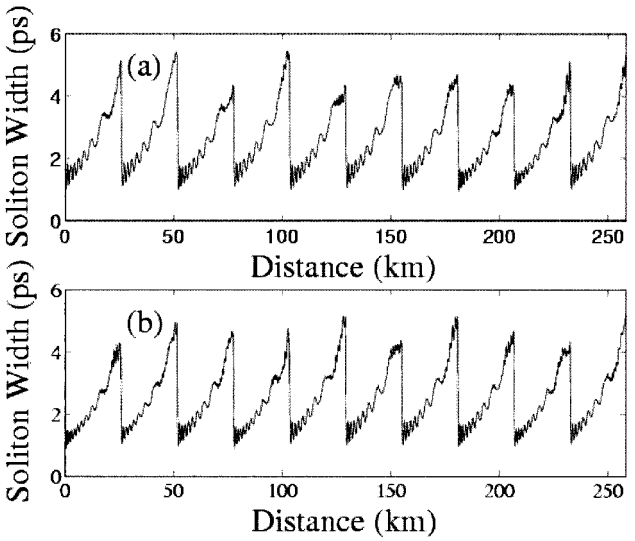

Fig. 10. Pulse width evolution under conditions identical to those of Fig. 9(b) except that the peak power of the input pulse to the first NALM is varied for (a) 487.4 mW and (b) 569.4 mW.

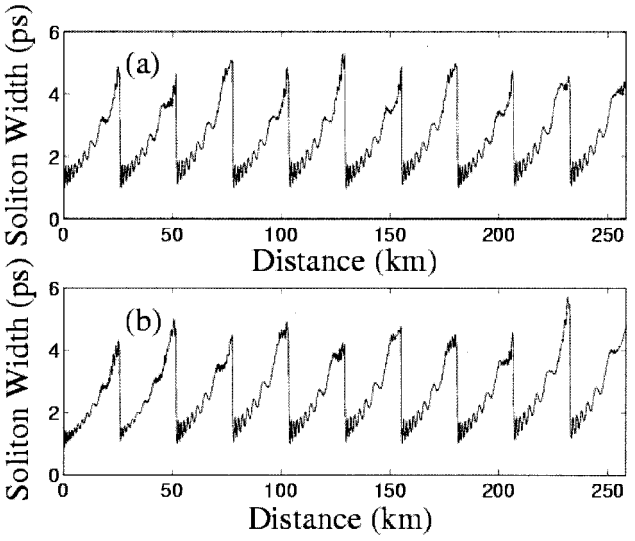

Fig. 11. Pulse width evolution under conditions identical to those of Fig. 9(b) except that the input pulse width to the first NALM is varied for (a) 4.71 ps and (b) 5.35 ps.

increases the average soliton width between two neighboring NALMs, both leading to a smaller spectrum shift.

Figure 9(b) shows the soliton spectra measured at the output of each NALM when both the RSS effect along the transmission fiber and the gain-dispersion effect within the NALM are considered, where the NALM, the input pulse, and the transmission fiber are identical to those used for Fig. 9(a) except that the loop-mirror spacing is decreased to 25.84 km to compensate for the gain-dispersion-induced energy loss. It is seen that, as compared with Fig. 9(a), the RSS-induced soliton self-frequency shift is suppressed by the gain-dispersion effect. For a transmission distance of 258.4 km, the center frequency shifts only by 150 GHz, which corresponds to a wavelength redshift of 1.2 nm if the center wavelength of the input pulse is 1550 nm.

D. Stability Analysis of the Transmission System

In practice, once the structure of the gain-distributed NALM and its spacing are fixed, stable soliton transmission should be maintained even with small variations of the initial pulse parameters such as amplitude and width. Fortunately, the NALM provides such a stabilization scheme because it provides a negative feedback mechanism for soliton transmission.[6,8] Figure 10 shows the evolution of the pulse width under conditions identical to those of Fig. 9(b) except that the peak power of the input pulse to the first NALM is varied for 487.4 mW [Fig. 10(a)] and 569.4 mW [Fig. 10(b)] (the input pulse width is fixed at 5 ps), which correspond to input soliton orders of 0.99 and 1.07, respectively. We see that stable transmission can be achieved over a relatively large range of the peak power of the input pulse. The evolution of the pulse width is similar to the case in a dispersion management system, but here no dispersion–compensation elements are used. Figure 11 shows pulse width evolution under conditions identical to those of Fig. 9(b) except that the input pulse width (FWHM) to the first NALM is varied for 4.71 ps [Fig. 11(a)] and 5.35 ps [Fig. 11(b)] (the peak power of the input pulse is fixed at 548.3 mW). Again, we see evolution patterns similar to those of Fig. 10.

The large stability range of the system benefits from the fact that the gain-distributed NALM has a broad switching window over which the quality of the transmitted pulse is very high. Comparing Fig. 3(b) with Figs. 1(b) and 2(b) we can see that the switching window of the gain-distributed NALM is nearly twice as broad as those of the conventional NALM and the NOLM and amplifier combination for the same gain of 10 dB. According to previous analysis,[8] the broader the switching window is the larger the stability range will be. Thus, for a similar loop-mirror spacing (or a similar gain), soliton transmission with gain-distributed NALMs should be more robust to small variations of the initial conditions than that with conventional NALMs or NOLM and amplifier combinations.

5. Conclusion

We have numerically shown that the amplifier spacing of a picosecond soliton transmission system can be significantly increased by use of gain-distributed NALMs instead of conventional NALMs or NOLM and amplifier combinations. The scheme is quite robust to variation of the initial conditions such as initial soliton power and width, which benefits from the fact that the gain-distributed NALM has a broad switching window over which the quality of the transmitted pulses is very high. We also show that soliton–soliton interactions can be reduced by using lowly dispersive fibers and that soliton self-frequency shift

can be suppressed by the gain-dispersion effect in the amplifying fiber loop.

This work was supported by the Research Grant Council of the Hong Kong Special Administrative Region of China under project PolyU5242/03E, by the National Natural Science Foundation of China under project 60277016, and by the Guangdong Natural Science Foundation of China under projects 021357 and 04011761.

References

1. G. P. Agrawal, *Fiber-Optic Communication Systems,* 3rd ed. (Wiley, 2002), pp. 404–477.
2. K. J. Blow and N. J. Doran, "Average soliton dynamics and the operation of soliton systems with lumped amplifiers," IEEE Photon. Technol. Lett. **3,** 369–371 (1991).
3. A. Hasegawa and Y. Kodama, "Guiding-center soliton in optical fibers," Opt. Lett. **15,** 1443–1445 (1990).
4. M. Nakazawa, K. Suzuki, H. Kubota, E. Yamada, and Y. Kimura, "Dynamic optical soliton communication," IEEE J. Quantum Electron. **26,** 2095–2102 (1990).
5. R. J. Essiambre and G. P. Agrawal, "Solution communication beyond the average-soliton regime," J. Opt. Soc. Am. B **12,** 2420–2425 (1995).
6. N. J. Smith and N. J. Doran, "Picosecond soliton transmission using concatenated nonlinear optical loop-mirror intensity filters," J. Opt. Soc. Am. B **12,** 1117–1125 (1995).
7. I. Gabitov, D. D. Holm, B. P. Luce, and A. Mattheus, "Recovery of solitons with nonlinear amplifying loop mirrors," Opt. Lett. **20,** 2490–2492 (1995).
8. I. Gabitov, D. D. Holm, and B. P. Luce, "Low-noise picosecond soliton transmission by use of concatenated nonlinear amplifying loop mirrors," J. Opt. Soc. Am. B **14,** 1850–1855 (1997).
9. Z. M. Liao, C. J. McKinstrie, and G. P. Agrawal, "Importance of prechirping in constant-dispersion fiber links with a large amplifier spacing," J. Opt. Soc. Am. B **17,** 514–518 (2000).
10. Y. Kominis and K. Hizanidis, "Nonlinear mode investigation in optical pulse propagation under periodic amplification and filtering," J. Opt. Soc. Am. B **20,** 545–553 (2003).
11. W. Cao and P. K. A. Wai, "Comparison of fiber-based Sagnac interferometers for self-switching of optical pulses," Opt. Commun. **245,** 177–186 (2005).
12. P. K. A. Wai and W. Cao, "Simultaneous amplification and compression of ultrashort solitons in an erbium-doped nonlinear amplifying fiber loop mirror," IEEE J. Quantum Electron. **39,** 555–561 (2003).
13. G. P. Agrawal, *Applications of Nonlinear Fiber Optics* (Academic, 2001), pp. 151–200.
14. M. Matsumoto, A. Hasegawa, and Y. Kodama, "Adiabatic amplification of solitons by means of nonlinear amplifying loop mirrors," Opt. Lett. **19,** 1019–1021 (1994).
15. K. Smith and L. F. Mollenauer, "Experimental observation of soliton interaction over long fiber paths: discovery of a long-range interaction," Opt. Lett. **14,** 1284–1286 (1989).
16. E. M. Dianov, A. V. Luchnikov, A. N. Pilipetskii, and A. N. Starodumov, "Electrostriction mechanism of soliton interaction in optical fibers," Opt. Lett. **15,** 314–316 (1990).
17. J. P. Gordon, "Theory of the soliton self-frequency shift," Opt. Lett. **11,** 662–664 (1986).
18. K. J. Blow, N. J. Doran, and D. Wood, "Suppression of the soliton self-frequency shift by bandwidth-limited amplification," J. Opt. Soc. Am. B **5,** 1301–1304 (1988).